Growth Factors and Stromal Matrix Proteins Associated with Mammographic Densities

Ya-Ping Guo, Lisa J. Martin, Wedad Hanna, Diponkar Banerjee, Naomi Miller, Eve Fishell, Rama Khokha, and Norman F. Boyd[1]

Division of Epidemiology and Statistics, Ontario Cancer Institute, Toronto, Ontario M5G 2 M9 [Y-P. G., L. J. M., N. F. B.]; Departments of Pathology [W. H.], and Radiology [E. F.], Sunnybrook and Women's College Hospital, Toronto, Ontario, M5S 1B2; Department of Pathology, Princess Margaret Hospital, Toronto, Ontario M5G 2 M9 [D. B., N. M., R. K.]; and Division of Experimental Therapeutics, Ontario Cancer Institute, Toronto, Ontario M5G 2 M9 [R. K.], Canada

Abstract

Extensive radiologically dense breast tissue is associated with a marked increase in breast cancer risk. To explore the biological basis for this association, we have examined the association of growth factors and stromal matrix proteins in breast tissue with mammographic densities. Ninety-two formalin-fixed paraffin blocks of breast tissues surrounding benign lesions were obtained, half from breasts with little or no density and half from breasts with extensive density, matched for age at biopsy. Sections were stained for cell nuclei, total collagen, the stromal matrix regulatory protein tissue metalloproteinase-3 (TIMP-3), and the growth factors, transforming growth factor-α and insulin-like growth factor (IGF-I). The area of immunoreactive staining was measured using quantitative microscopy. Breast tissue from subjects with extensive densities had a greater nuclear area ($P = 0.007$), as well as larger stained areas of total collagen ($P = 0.003$), TIMP-3 ($P = 0.08$), and IGF-I ($P = 0.02$) when compared with subjects with little breast density. Differences were greater for subjects less than 50 years of age. These data indicate that increased tissue cellularity, greater amounts of collagen, and increased IGF-I and TIMP-3 expression are found in tissue from mammographically dense breasts and suggest mechanisms that may mediate the associated increased risk of breast cancer.

Introduction

There is marked variation between individuals in the radiological appearance of the breast that is attributable to variations in tissue composition. Fat is radiolucent and appears dark on a mammogram, whereas stroma and epithelium are radio-dense and appear light, an appearance that we refer to in this study as mammographic densities (1). Studies that have used quantitative methods to classify mammographic densities have consistently found that women with dense tissue in more than 60–75% of the breast are at four to six times greater risk of breast cancer than women with no density (2).

A total of nine studies have been published that have used quantitative methods to classify mammographic densities (2). All of them found significantly elevated odds ratios between extreme categories of density. Although mammographic density is associated with several known risk factors for breast cancer, all of the studies controlled for at least some risk factors for breast cancer, and all of them found that mammographic density was associated with breast cancer risk after adjustment for other risk factors. It has been proposed that the increased risk of breast cancer is an artifact, created by the recognized difficulty in detecting cancer in dense tissue. However, in subjects reexamined over an extended period of time, any effects of masking will be short-lived, because cancers missed at one examination will be detected at subsequent examinations (3). Among the eight published studies are two large nested case-control studies performed in cohorts that were screened at annual intervals for several years. Both showed that the increased risk of breast cancer associated with dense breast tissue persisted for extended periods of time, one for at least 5 years and the other for at least 10 years. A more detailed discussion of these issues has been given elsewhere (2). The biological basis for the increase in risk associated with radiologically dense breast tissue is, however, not known.

Studies of the histological features of the breast associated with variations in radiological appearance have found that mammographic densities are associated with proliferation of either stroma or epithelium (2), the two types of tissue in the breast with X-ray attenuation characteristics that give rise to radiologically dense breast (1). On the basis of a general model of carcinogenesis proposed by Shigenaga and Ames (4), we propose that the combined effects of two processes, cell proliferation (mitogenesis) and damage to the DNA of dividing cells by endogenous mutagens (mutagenesis; Ref. 5), underlie the risk of breast cancer associated with mammographically dense breast tissue.

The mammary epithelium, stromal fibroblasts, and myoepithelial cells communicate by means of several paracrine signals (6–8), and we hypothesize that growth factors within the stroma influence stromal cell proliferation and matrix deposition, which contribute to mammographically dense breast tissue and either directly or indirectly affect the epithelium. In this study, we have examined the quantity of cell nuclei, collagen, and selected molecular factors in breast tissue in relation to mammographic densities. Compared with tissue from breasts with little radiological density, we found significantly greater

Received 6/9/00; revised 12/14/00; accepted 12/26/00.
The costs of publication of this article were defrayed in part by the payment of page charges. This article must therefore be hereby marked *advertisement* in accordance with 18 U.S.C. Section 1734 solely to indicate this fact.
[1] To whom requests for reprints should be addressed, at Division of Epidemiology and Statistics, Ontario Cancer Institute, 610 University Avenue, Toronto, Ontario M5G 2 M9, Canada. Phone: (416) 946-2945; Fax (416) 946-2024; E-mail: boyd@oci.utoronto.ca.

nuclear area, area of collagen, and stained areas of IGF-I[2] and TIMP-3 in tissue from radiologically dense breasts.

Materials and Methods

Preliminary Work. In preliminary work, tissue blocks from subjects with little and extensive mammographic density were selected without matching for age and stained with antibodies to the following factors: collagen type IV, total collagen (Masson trichrome), Tenascin, VEGF, IGF-I, TGF-α, and TIMP-3. A total of 103 blocks were selected, and an average of 34 blocks from subjects with little density and an approximately equal number from women with extensive densities were examined for each of the factors examined. (For TIMP-3, only 22 and 25 blocks were examined, respectively, from women with nondense and dense breast tissue). When we compared the area of staining in tissue from dense and nondense breasts, we found that total collagen ($P = 0.0001$), IGF-I ($P = 0.02$), TGF-α ($P = 0.04$), and TIMP-3 ($P = 0.11$) showed evidence of an association with mammographic density. No association was found with collagen type IV ($P = 0.38$), Tenascin ($P = 0.57$), or VEGF ($P = 0.80$). Total collagen, IGF-I, TGF-α, Tenascin, and TIMP-3 were all also significantly and negatively correlated with age ($r = -0.30$ to -0.42). VEGF and collagen type IV were not correlated with age.

Because of the strong inverse association with age found for the factors that also differed between women with and without extensive mammographic densities, we carried out the study reported here to examine the relation of these factors to mammographic density in tissue sections from age-matched pairs of subjects.

General Method. Tissue sections from 92 formalin-fixed paraffin blocks of tissues surrounding benign lesion were examined, half from breasts with little or no mammographic density and half from breasts with extensive densities. Subjects with dense and nondense breast tissue were matched individually according to age at the time of biopsy within 2 years. Tissue sections were stained for cell nuclei, total collagen, and antibodies to selected growth factors and stromal regulatory proteins. The stained area for each marker was measured using quantitative microscopy, and the areas labeled with various antibodies were used to compare different growth factors in breast tissue with different radiological characteristics.

Selection of Material. The histological sections that are the subject of the present study were selected from a computerized list of 422 women having fine needle localization biopsies of the breast at Women's College Hospital, Toronto, Ontario, Canada between January 4, 1987 and October 15, 1997. In these women, the histological findings on biopsy were nonmalignant. This material allowed a radiological classification of both the whole breast and the region of the breast from which the biopsy was taken. A classification of the extent of radiological density in the mammogram was made as part of routine reporting, and we selected those with either less than 25% or more than 50% of the image occupied by dense tissue.

Subjects with extensive densities were identified first and then matched individually to subjects with little density, according to age within 2 years at the time of biopsy. When more than one match was available, the pair of subjects with the closest date of biopsy was selected. The pathology reports of breast biopsies from the subjects selected were reviewed, and a tissue block remote from any discrete lesion was selected for the preparation of histological sections. A total of 49 pairs of subjects met these criteria for matching, and we were able to obtain tissue blocks from 46 of these subjects. Eighteen of the 46 pairs had also been used in the preliminary work described above. The date of biopsy differed between members of the matched pairs by an average of 1.7 years (SD, 3.8 years).

Other than age, no information was available about the subjects, and thus menopausal status and the phase of the menstrual cycle at which the mammogram and biopsy were done were unknown.

Antibodies. The antibodies used were as follows: (*a*) For primary antibodies, mouse antihuman TGF-α, a monoclonal antibody (GF10; Oncogene Science), was used in a working dilution of 1:40. Mouse antihuman IGF-I monoclonal antibody (05-172; Upstate Biotechnology, Inc.) and rabbit TIMP-3 polyclonal antibody were used in a working dilution of 1:5. ngIR (Triple Point Biologics) was used in a working dilution of 1:1000; (*b*) for secondary antibodies, biotinylated goat antimouse IgG (62-6540; Zymed) was used for the IGF-I and TGF-α, and biotinylated goat antirabbit IgG (62-6140; Zymed) was used for TIMP-3. Both antibodies were used in a working dilution of 1:200; (*c*) streptavidin-horseradish peroxidase (P0397; DAKO) was used in a working dilution of 1:300.

Immunohistochemical Staining. Serial sections were cut from each block, 3 μm in thickness, and mounted on *N*-tris(hydroxymethyl)methyl-2-aminoethanesulfonic acid-coated slides (12-550-15; Fisher Scientific). Sections were first incubated at room temperature with primary antibodies for 1 h for IGF-1 and TGF-α or overnight for TIMP-3. After washes in PBS, the sections were incubated with secondary antibodies for 30 min at room temperature and then with streptavidin for 30 min at room temperature. Growth factors labeled with antibodies were visualized by incubation with 3-amino-9-ethyl-carbazole (A6926; Sigma Chemical Co.), which gives a red color in the presence of horseradish peroxidase. Nuclei in the sections were stained by hematoxylin.

Total collagen was stained by Masson trichrome. The slides were mounted with Crystalmount (M03; Biomeda) and dried in the air, and coverslips were secured with Permount (SP15–500; Fisher Scientific).

Quantitative Microscopy. All of the measurements were made without knowledge of the radiological characteristics of the breast from which the biopsy was taken. Nuclear areas were chosen to represent the density of cellularity in each section. Measurements were made using a Zeiss Axioskop light microscope fitted with a JVC ky-17 series 3-CCD color video camera, interfaced to a SAMBA 4000 Image Analysis System with a Matrox 640-frame grabber board (Image Products International, Inc., Chantilly, VA). A $31.25 \times (25 \times 1.25)$ objective lens yielded an image size of 155 μmm $\times$ 114.5 μmm or 17747.5 μmm^2/camera field of view. The threshold was set to segment total areas, including both nuclear area and antibody-labeled area, from background. The hue histogram was used to distinguish antibody-labeled area (red color) from total labeled area and is illustrated in Fig. 1 for IGF-I. The data for both areas were tracked separately on the SAMBA system. The antibody-labeled area for each molecular factor was then calculated from the total stained area minus the nuclear area. Because nuclear staining (hematoxylin) and total collagen (Masson trichrome) could not be separated by the SAMBA system, their combined stained area was measured on one slide, and the area of collagen staining was then calculated by subtracting the nuclear area measured on a separate slide.

For each section, the total nuclear area and the total antibody-labeled area were calculated from 80 fields. Eighty fields

[2] The abbreviations used are: IGF, insulin-like growth factor, TIMP-3, tissue metalloproteinase-3; VEGF, vascular endothelial growth factor; TGF-α, transforming growth factor-α.

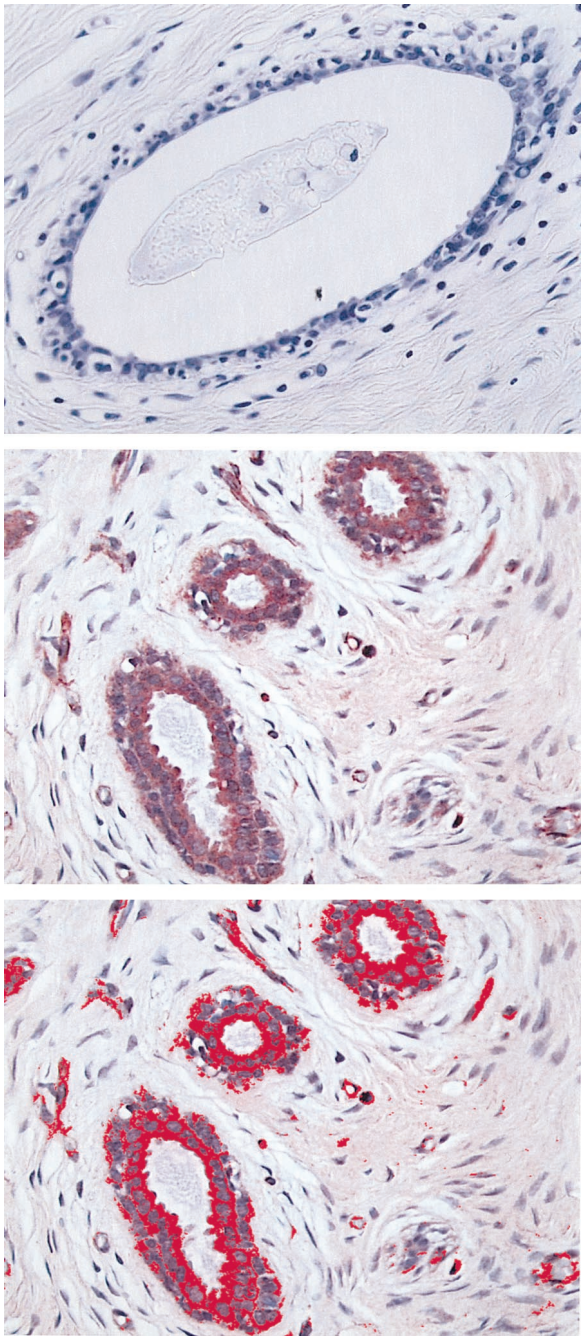

Fig. 1. Image analysis. *Top*, negative control for IGF-I staining; *middle*, IGF-I staining; *bottom*, IGF-I-stained area outlined in *red* by thresholding. All of the images are shown at ×40 magnification.

in each section were randomly selected along the track starting from the top spot of the section. Every second or third field on the track was selected so that the entire section would be covered by these 80 fields. The method used to select fields to be measured in a section is illustrated in Fig. 2.

Pathology and Radiology Review. One section from each of the blocks selected for immunohistochemistry was reviewed and classified according to their histological appearance. The mammogram used for classification was the film taken in association

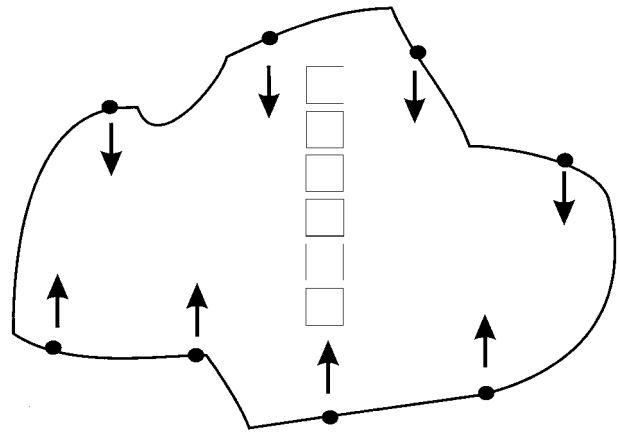

Fig. 2. Measurement of the selection of fields. Illustration of the method used to select fields to be measured. Eighty fields in each section were randomly selected along the track starting from the top of the section. Every second or third field on the track was selected so that the entire section could be covered by these eighty fields.

with the needle localization procedure at the time of biopsy. These mammograms were reviewed and classified according to the extent of density in the entire image, using six categories (0%, <10%, <25%, <50%, <75%, and >75%), and also according to the presence of fatty tissue or radiologically dense breast tissue at the site of the biopsy.

Statistical Analysis. The area of staining for each growth factor and nuclear area of each slide was calculated by dividing the areas labeled with antibody by the total analysis area and was expressed as a percentage. Because a measure of nuclear area was available from all of the slides, an average was calculated from all of the slides for each subject and used in the comparisons shown. The distributions for growth factors and nuclear area were highly skewed. These distributions were improved by log transformation, but not all of them were normalized. For statistical analysis, the difference between high and low density members of each matched pair in the logarithm of the percentage of the measured area stained for nuclear area, collagen, growth factors, and stromal proteins was calculated. The paired differences of the log-transformed values were normally distributed and were compared between breasts of low and high mammographic density using the paired *t* test (two-sided). The distribution of growth factors from dense and fatty biopsy sites were compared using the Wilcoxon two sample test (unpaired).

Results

Characteristics of Subjects. Selected characteristics of the subjects studied are given in Table 1. The median age was 48.5 years for subjects with low density and 49.0 years for subjects with extensive radiological density. Of subjects with low density, 15.2% had no density, and 30.4% had density in more than 10% but less than 25% of the breast. Of subjects with high density, 82.6% had more than 75% of the breast occupied by radiologically dense tissue, and 97.8% had dense tissue in more than 50% of the breast. The histological classification of the biopsies from these subjects is shown in Table 1. In subjects with low density, the most common classifications were nonproliferative fibrocystic change (50.0%) and "normal" (21.7%). In subjects with extensive densities, the most common histological classifications were proliferative fibrocystic change without atypia (45.7%) and nonproliferative fibrocystic change (37.0%).

Table 1 Selected characteristics of subjects

	Low density (n = 46)	High density (n = 46)
Median age	48.5	49.0
Interquartile range	(45–55)	(45–55)
Radiological classification (No. of subjects)		
0% density	7	0
>0–<10% density	24	0
10–25% density	14	0
25–50% density	0	1
50–75% density	0	7
>75% density	0	38
Missing	1	0
Histological classification (No. of subjects)		
Normal	10	1
Stromal fibrosis	4	5
Nonproliferative, fibrocystic change	23	17
Proliferative FCC[a] without atypia	8	21
Proliferative FCC with atypia	0	1
Not assessed/missing	1 (fibroadenoma)	1 (missing)

[a] FCC, fibrocystic change.

Relationship of Immunohistochemical Staining with Mammographic Densities. Table 2 shows the mean of the log-transformed values for the percentage area of each variable from 46 age-matched pairs of subjects with little density or extensive density, as well as the mean difference from the comparison of age-matched pairs. All of the statistical comparisons and the percentage differences referred to below are based on the mean paired differences.

Each of the parameters measured with the exception of TGF-α, which was similar in the two groups, was substantially greater in tissue from subjects with extensive mammographic densities than in those with little density. The paired difference between low- and high-density subjects in log-transformed mean nuclear area was about twice the mean for low-density subjects. The mean difference in stained area of total collagen was about 50% greater than the low-density value; the mean difference in the areas of staining for IGF-I was about twice the low-density value, and the difference for TIMP-3 was about equal to the low-density value.

Table 3 shows the results separately for the 24 pairs of subjects less than 50 years of age whose mean age was 44 years and for the 22 pairs of subjects 50 or more years of age whose mean age was 57 years. In younger subjects (Table 3*A*), the paired difference between low- and high-density subjects in log-transformed mean nuclear area was about 17 times greater than the mean for low-density subjects. The mean difference in stained area of total collagen was about twice the low-density value; the mean difference in area of staining for IGF-I about three times greater than the low-density value, and the mean difference in the area of TIMP-3 staining was about twice the low-density value. Stained areas of TGF-α were similar in the two groups.

In older subjects (Table 3*B*), only the difference in collagen approached statistical significance and was greater in those with more extensive radiologically dense tissue. Nuclear area and stained areas of TGF-α and TIMP-3 were all slightly less, and the area of IGF-I slightly greater, in those with extensive densities than in subjects with less density, but none of these differences was statistically significant. No correlation was found between the area of staining for any antibody and age (data not shown).

Relationship of Immunohistochemical Staining with Mammographic Densities at the Site of Biopsy. Table 4 shows the relationship of immunohistochemical staining to the presence or absence of mammographic density at the site of biopsy. There was a strong relationship between the radiological density in the breast as a whole and density at the biopsy site. In 82% of biopsies from high-density breasts, there was density at the site of biopsy. In 87% of biopsies from low-density breasts, the biopsy site was nondense, and radiological features such as calcification or a localized mass were present. The analysis shown in Table 4 had to be carried out without reference to the matched pairs. The data were again highly skewed and could not be normalized by log transformation, and median values are shown in the table. Log-transformed mean values are also shown in the table to allow comparison with the values in Tables 2 and 3. The statistical comparisons shown are (two-sided) Wilcoxon tests of the distributions within each group. Biopsies from areas of the breast that were radiologically dense had a nuclear area more than double that of biopsies from fatty regions. The stained area for total collagen was three times greater in biopsies from dense areas, and the area of IGF-I staining was almost twice as great. Smaller and statistically nonsignificant differences were seen for TGF-α and TIMP-3.

Discussion

An association between radiologically dense breast tissue and an increased risk of breast cancer was first described by Wolfe (9–10), and at least 15 other studies have confirmed that Wolfe's qualitative classification is associated with risk of breast cancer (5). In addition, nine studies to date have used quantitative approaches to reach a similar conclusion. All of these studies found increased risk associated with more extensive density, and all of them but one found a risk of four or greater in women with extensive mammographic density compared with those with little density. This gradient in risk is larger than is found with most other risk factors for breast cancer. However, the biological basis of the association of mammographic density with risk of breast cancer has not been explained.

In this study, we report that mammographically dense breast tissue is associated with an increased number of cells and an increased amount of collagen. In addition, we show that greater amounts of the growth factor IGF-I and the stromal matrix regulatory protein TIMP-3 were present in tissue from radiologically dense breasts. The mammogram used to classify the overall density of the breast in the analyses shown here was taken at the time of biopsy, in association with the needle localization procedure, and thus was taken at exactly the same time as the biopsy. Because density in the breast as a whole and density at the site of biopsy were strongly associated, we are not able to examine separately the associations of factors with dense tissue in a breast that is predominately radiologically nondense or with nondense tissue in a breast that is mainly dense.

These results are consistent with our hypothesis that the stromal and epithelial proliferation that contributes to mammographically dense breast tissue is associated with the presence of specific growth regulatory factors. We propose that IGF-I and TIMP-3 may influence both the formation of the tissues responsible for mammographic densities and the associated risk of breast cancer.

Two types of tissue in the breast, stroma and epithelium, have X-ray attenuation characteristics that are responsible for

Table 2 Comparison of molecular factors in tissue from breasts with low density and high density ($n = 46$ age matched pairs)

	Low density[a]	High density[a]	Difference (low-high)[b]	P[c]
Percentage of nuclear area ($n = 46$)	0.27[a] (0.89)	0.85 (0.91)	−0.58 (1.40)	0.007
Percentage of total collagen[d] ($n = 41$)	2.21 (1.66)	3.32 (1.56)	−1.11 (2.27)	0.003
Percentage of IGF-1[e] ($n = 45$)	−0.29 (1.82)	0.48 (1.37)	−0.77 (2.15)	0.02
Percentage of TGF-α[e] ($n = 45$)	−1.36 (2.05)	−1.49 (2.24)	0.12 (2.87)	0.77
Percentage of TIMP-3 ($n = 46$)	−0.99 (2.47)	−0.12 (2.49)	−0.86 (3.27)	0.08

[a] Results expressed as mean (SD) of log-transformed values.
[b] Paired differences (low-high density log-transformed value) expressed as mean (SD).
[c] P for t-test for paired difference.
[d] Values missing because of sections unsuitable for staining ($n = 2$) and staining measurement problems ($n = 2$).
[e] Value missing because of sections unsuitable for staining ($n = 1$ for each measure).

Table 3 Comparison of molecular factors in tissue from breasts with low and high breast density in women < and ≥ 50 years of age

	Low density[a]	High density[a]	Difference (low-high)[b]	P[c]
A. Women <50 years of age; $n = 24$ pairs; mean age = 44 years				
Percentage of nuclear area	0.07[a] (0.84)	1.23 (0.80)	−1.17 (1.16)	0.0001
Percentage of total collagen ($n = 22$)	1.76 (1.86)	3.17 (1.83)	−1.41 (2.64)	0.02
Percentage of IGF-1	−0.42 (1.42)	0.89 (1.05)	−1.31 (1.69)	0.0009
Percentage of TGF-α	−1.53 (1.81)	−1.34 (2.49)	−0.19 (2.95)	0.75
Percentage of TIMP-3	−1.54 (2.21)	0.52 (2.22)	−2.06 (3.17)	0.004
B. Women ≥50 years of age; $n = 22$ age matched pairs; mean age = 57 years				
Percentage of nuclear area	0.49 (0.91)	0.42 (0.85)	0.07 (1.36)	0.82
Percentage of total collagen ($n = 19$)	2.80 (1.24)	3.32 (0.96)	−0.76 (1.77)	0.08
Percentage of IGF-1 ($n = 21$)	−0.14 (2.22)	0.02 (1.57)	−0.16 (2.48)	0.78
Percentage of TGF-α ($n = 21$)	−1.17 (2.32)	−1.65 (1.95)	0.49 (2.81)	0.44
Percentage of TIMP-3	−0.38 (2.65)	−0.83 (2.63)	0.45 (2.90)	0.48

[a] Results expressed as mean (SD) of log-transformed values.
[b] Paired difference (low-high density log-transformed value) expressed as mean (SD).
[c] P for t test for paired difference.

Table 4 Comparison of molecular factors in tissue from biopsies taken from fatty and dense sites (unpaired)

	Fatty tissue at biopsy site	Dense tissue at biopsy site	P[a]
Percentage of nuclear area	1.01 (0.54–2.33)[b]	2.52 (1.06–5.00)	0.0004
	0.17[c]	*0.87*	
	$n = 40$	$n = 51$	
Percentage of total collagen	11.69 (3.49–33.48)	35.54 (10.98–62.70)	0.002
	2.14	*3.02*	
	$n = 35$	$n = 48$	
Percentage of IGF-1	1.13 (0.21–2.64)	1.94 (0.75–4.06)	0.05
	−0.32	*0.44*	
	$n = 40$	$n = 50$	
Percentage of TGF-α	0.30 (0.06–0.81)	0.42 (0.11–1.32)	0.30
	−1.70	*−1.21*	
	$n = 39$	$n = 51$	
Percentage of TIMP-3	0.45 (0.05–3.63)	0.54 (0.06–5.93)	0.45
	−0.81	*−0.39*	
	$n = 40$	$n = 51$	

[a] P for two sample Wilcoxon tests comparing median values.
[b] Median (interquartile range) of untransformed values.
[c] Mean of log-transformed data in italics to allow comparison with Tables 2 and 3.

radiologically dense breast tissue (11). Several studies (12–19) have examined the relationship between histological and radiological features of the breast, and all of them have found an association between mammographic density and proliferation of stroma, epithelium, or both. The studies of Bartow *et al.* (20–22) and Hart *et al.* (23), which are based on forensic autopsy material and are, therefore, unique in that there was no selection of subjects or histological material for the presence of breast disease, also showed that the more dense Wolfe's patterns had increasing fibrosis. Therefore, proliferation of epithelium or parenchyma are common events in the breast tissue, and a knowledge of the factors contributing to this proliferation is crucial to our understanding of the relation of these features of breast tissue to risk of breast cancer.

IGF-I is a known mitogen for breast epithelium and is produced in the breast stroma as well as in the liver. Several components of the IGF system, including IGF peptides, IGF-binding proteins, and the receptor through which IGFs exert their mitogenic signal, have been shown to be dysregulated in breast cancer, suggesting a role of IGFs in the genesis of breast cancer (24, 25). In the current investigation, we found significantly greater areas positive for IGF-I immunostaining in tissues from mammographically dense breasts. This suggests that an up-regulation of IGF-I may be an early event related to the risk of developing breast cancer.

Higher circulating levels of IGF-I have been found in a prospective cohort study (26) to be associated with an increased risk of breast cancer in premenopausal but not in postmenopausal women. Higher levels of circulating IGF-I have also been found to be associated with mammographic densities in premenopausal but not in postmenopausal women (27). These associations between menopausal status and IGF-I levels may be related to the finding in the present study that greater areas of IGF-I staining, as well as a larger area of stained nuclei, were associated with mammographic densities only in women under the age of 50 years. In women over the age of 50, only the stained area of collagen was associated with density. The differences in the association of mammographic densities and molecular factors seen in women under and over 50 should be interpreted with caution, because this

was a *post hoc* analysis and the sample sizes are small. This observation warrants further study. However, the associations of higher blood levels of IGF-I with increased risk of breast cancer and with mammographic densities have also, as noted above, been found only in younger women.

The mechanism that associates the amount of collagen to risk of breast cancer is uncertain, but collagen production is often a conspicuous feature of breast cancer (through unknown mechanisms), and interactions between stroma and epithelium are known to be important in organogenesis and carcinogenesis in the breast (6–8). Opposing actions of matrix-degrading matrix metalloproteinases and their tissue inhibitors, TIMPs, largely determine the extent of stromal matrix degradation. Traditionally, matrix has been viewed as an ultrastructure of molecules capable of providing support for cells and tissues. However, it is now realized that in addition to providing supportive architecture, the matrix can influence proliferation, apoptosis, and migration (28–31). Therefore, the observed up-regulation of TIMP-3 immunostaining may influence matrix deposition, which in turn will affect breast tissue density. Further, because we have shown in other work that a TIMP can directly affect the bioavailability of a growth factor such as IGF-II, it is possible that TIMP-3 may have a dual effect (32). Beyond influencing matrix deposition, it may alter bioactivity of IGFs in dense breast tissue.

Although the present study has identified factors associated with mammographically dense breast tissue, the number of subjects studied was limited by the availability within a single institution of matched pairs of tissue samples from subjects with extreme differences in mammographic densities. Study of a larger number of samples will be required to determine whether the associations that we describe here are a local phenomenon, associated only with tissue at the site of biopsy, or are a feature of the breast as a whole. Preferably, the material for such a study should not have been selected for the presence of suspected breast disease, the autopsy series referred to above would be suitable for this purpose, and information about menopausal status and phase of the menstrual cycle would be available. Further, the number of growth factors and stromal regulatory proteins that we had resources to examine in this study was also limited, and additional study is warranted of other influences suggested by the biological rationale given above.

Acknowledgments

The authors thank Trudey Nicklee for her excellent assistance and support during image analysis on the SAMBA system. We also thank James Ho and Barbara Terrett for their help on the immunohistochemical staining of sections.

References

1. Ingleby, H., and Gerson-Cohen, J. Comparative Anatomy, Pathology and Roentgenology of the Breast. Philadelphia: University of Philadelphia Press, 1960.

2. Boyd, N. F., Lockwood, G. A., Byng, J., Tritchler, D. L., and Yaffe, M. Mammographic densities and breast cancer risk. Cancer Epidemiol. Biomark. Prev., *7:* 1133–1144, 1998.

3. Whitehead, J., Carlile, T., Kopecky, K. J., Thompson, D. J., Gilbert, F. I., Jr., Present, A. J., Threatt, B. A., Krook, P., and Hadaway, E. Wolfe mammographic parenchymal patterns: a study of the masking hypothesis of Egan and Mosteller. Cancer (Phila.), *56:* 1280–1286, 1985.

4. Shigenaga, M. K., and Ames, B. N. Oxidants and mitogenesis as causes of mutation and cancer: the influence of diet. Basic Life Sci., *61:* 419–436, 1993.

5. Boyd, N., Lockwood, G., Martin, L. J., Knight, J. A., Byng, J., Yaffe, M., and Tritchler, D. Mammographic densities and breast cancer risk. Breast Dis., *10:* 113–126, 1998.

6. Cullen, K. J., and Lippman, M. E. Stromal-epithelial interactions in breast cancer. *In:* R. B. Dickson and M. E. Lippman (eds.), Genes, Oncogenes and Hormones: Advances in Cellular and Molecular Biology of Breast Cancer, pp. 413–431. Boston: Kluwer Associates, 1991.

7. Dickson, R. B., and Lippman, M. E. Growth factors in breast cancer. Endocr. Rev., *16:* 559–589, 1995.

8. Sakakura, T. New aspects of stroma-parenchyma relations in mammary gland differentiation. Int. Rev. Cytol., *125:* 165–202, 1991.

9. Wolfe, J. N. Breast patterns as an index of risk for developing breast cancer. Am. J. Roentgenol., *126:* 1130–1139, 1976.

10. Wolfe, J. N. Risk for breast cancer development determined by mammographic parenchymal pattern. Cancer (Phila.), *37:* 2486–2492, 1976.

11. Johns, P. C., and Yaffe, M. J. X-ray characterization of normal and neoplastic breast tissues. Phys. Med. Biol., *32:* 675–695, 1987.

12. Arthur, J. E., Ellis, I. O., Flowers, C., Roebuck, E., Elston, C. W., and Blamey, R. W. The relationship of high risk mammographic patterns to histological risk factors for development of cancer in the human breast. Br. J. Radiol., *63:* 845–849, 1990.

13. Bland, K. I., Kuhns, J. G., Buchanan, J. B., Dwyers, P. A., Heuser, L. F., O'Connor, C. A., Gray, S. A., Sr., and Polk, H. C., Jr. A clinicopathologic correlation of mammographic parenchymal patterns and associated risk factors for human mammary carcinoma. Ann. Surg., *195:* 582–594, 1982.

14. Boyd, N. F., Jensen, H., Cooke, G., and Lee Han, H. W. Relationship between mammographic and histological risk factors for breast cancer. J. Natl. Cancer Inst. (Bethesda), *84:* 1170–1179, 1992.

15. Bright, R., Morrison, A., Brisson, J., Burstein, N., Sadowsky, N., Kopans, D., and Meyer, J. Relationship between mammographic and histologic features of breast tissue in women with benign biopsies. Cancer (Phila.), *61:* 266–271, 1988.

16. Fisher, E., Palekar, A., Kim, W., and Redmond, C. The histopathology of mammographic patterns. Am. J. Clin. Pathol., *69:* 421–426, 1978.

17. Moskowitz, M., Gartside, P., and McLaughlin, C. Mammographic patterns as markers for high-risk benign breast disease and incidence cancers. Radiology, *134:* 293–295, 1980.

18. Urbanski, S., Jensen, H. M., Cooke, G., McFarlane, D., Shannon, P., Kruikov, V., and Boyd, N. F. The association of histological and radiological indicators of breast cancer risk. Br. J. Cancer, *58:* 474–479, 1988.

19. Wellings, S. R., and Wolfe, J. Correlative studies of the histological and radiographic appearance of the breast parenchyma. Radiology, *129:* 299–306, 1978.

20. Bartow, S. A., Mettler, F. A., Jr., and Black, III, W. C. Correlations between radiographic patterns and morphology of the female breast. Rad. Patterns Morph., *13:* 263–275, 1997.

21. Bartow, S. A., Pathak, D. R., Black, W. C., Key, C. R., and Teaf, S. R. Prevalence of benign, atypical and malignant breast lesions in populations at different risk for breast cancer. A forensic autopsy study. Cancer (Phila.), *60:* 2751–2760, 1987.

22. Bartow, S. A., Pathak, D. R., Mettler, F. A., Key, C. R., and Pike, M. C. Breast mammographic pattern: a concatenation of confounding and breast cancer risk factors. Am. J. Epidemiol., *142:* 813–819, 1995.

23. Hart, B. L., Steinbock, R. T., Mettler, Jr., F. A., Pathak, D. R., and Bartow, S. A. Age and race related changes in mammographic parenchymal patterns. Cancer (Phila.), *63:* 2537–2539, 1989.

24. Rasmussen, A. A., and Cullen, K. J. Paracrine/autocrine regulation of breast cancer by the insulin-like growth factors. Breast Cancer Res. Treat., *47:* 219–233, 1998.

25. Rudland, P. S., Fernig, D. G., and Smith, J. A. Growth factors and their receptors in neoplastic mammary glands. Biomed. Pharmacother., *49:* 389–399, 1995.

26. Hankinson, S. E., Willet, W. C., Colditz, G. A., Hunter, D. J., Michaud, D. S., Deroo, B., Rosner, B., Speizer, F. E., and Pollak, M. Circulating concentrations of insulin-like growth factor-I and risk of breast cancer. Lancet, *351:* 1393–1396, 1998.

27. Byrne, C., Colditz, G. A., Willet, W. C., Speizer, F. E., Pollak, M., and Hankinson, S. E. Plasma insulin-like growth factor (IGF) I, IGF-binding Protein 3, and mammographic density. Cancer Res., *60:* 3744–3748, 2000.

28. Giannelli, G., Falk-Marzillier, J., Schiraldi, O., Stetler-Stevenson, W. G., and Quaranta, V. Induction of cell migration by matrix metalloprotease-2 cleavage of laminin-5. Science (Washington DC), *277:* 225–228, 1997.

29. Hay, E. D. Extracellular matrix alters epithelial differentiation. Curr. Opin. Cell Biol., *5:* 1029–1035, 1993.

30. Lin, C. Q., and Bissell, M. J. Multi-faceted regulation of cell differentiation by extracellular matrix. FASEB J., *7:* 737–743, 1993.

31. Martin, D. C., Ruther, U., Sanchez-Sweatman, O. H., Orr, F. W., and Khokha, R. Inhibition of SV40 T antigen-induced hepatocellular carcinoma in TIMP-1 transgenic mice. Oncogene, *13:* 569–576, 1996.

32. Martin, D. C., Fowlkes, J. L., Babic, B., and Khokha, R. Insulin-like growth factor II signaling in neoplastic proliferation is blocked by transgenic expression of metalloproteinase inhibitor TIMP-I. J. Cell Biol., *146:* 881–892, 1999.

Growth Factors and Stromal Matrix Proteins Associated with Mammographic Densities

Ya-Ping Guo, Lisa J. Martin, Wedad Hanna, et al.

Cancer Epidemiol Biomarkers Prev 2001;10:243-248.